Inorg. Chem. **1991,** *30,* 2623-2630

Contribution from the Department of Chemistry,
University of Rochester, Rochester, New York 14627

Synthesis and Characterization of Mono- and Bis(silyl)iridium Bis(phosphine) Complexes

Mary K. Hays and Richard Eisenberg*

Received August 21, 1990

The trihydride complex $IrH_3(CO)(dppe)$ (dppe = 1,2-bis(diphenylphosphino)ethane) reacts with primary, secondary, and tertiary silanes to yield mono- and bis(silyl) hydride complexes of the formulas $IrH_2(SiRR'_2)(CO)(dppe)$ (**1**) and $IrH(SiRR'_2)_2(CO)(dppe)$ (**2**). The different silanes used include Ph_3SiH, Et_3SiH, Me_3SiH, Me_2ClSiH, $MeCl_2SiH$, Ph_2SiH_2, Me_2SiH_2, $PhSiH_3$, and $EtSiH_3$. The reactions were monitored by ^1H NMR and ^{31}P NMR spectroscopies, which allow unambiguous assignment of the coordination geometries of the products. For the mono(silyl) dihydride systems **1**, the hydrides are cis to each other with one trans to CO and the other trans to P; the silyl ligand is trans to the remaining P. The complex $IrH_2(SiMe_3)(CO)(dppe)$ (**1c**) catalyzes hydrosilation and dehydrogenative silylation of ethylene, albeit slowly. For the bis(silyl) complexes **2**, the silyl groups are equivalent and trans to the dppe P donors. The structures of the bis(silyl) complexes $IrH(SiClMe_2)_2(CO)(dppe)$ (**2d**) and $IrH(SiHMe_2)(SiClMe_2)(CO)(dppe)$ (**2j**) have been determined by single-crystal X-ray diffraction methods. For **2d**, $a = 12.952$ (2) Å, $b = 15.480$ (5) Å, $c = 9.567$ (2) Å, $\alpha = 100.58$ (2)°, $\beta = 111.55$ (1)°, $\gamma = 105.73$ (2)°, space group $P\bar{1}$, $Z = 2$, $R = 0.029$, and $R_w = 0.041$. For **2j**, $a = 11.976$ (5) Å, $b = 15.816$ (9) Å, $c = 9.357$ (3) Å, $\alpha = 93.43$ (4)°, $\beta = 110.01$ (3)°, $\gamma = 77.59$ (4)°, space group $P\bar{1}$, $Z = 2$, $R = 0.035$, and $R_w = 0.046$. The structures of both complexes confirm the coordination geometry assigned on the basis of the spectroscopy. The complex $IrH(SiH_2Et)_2(CO)(dppe)$ was observed to react rapidly with $BF_3{\cdot}Et_2O$ leading to formation of the bis(fluorosilyl) complex $IrH(SiEtF_2)_2(CO)(dppe)$ (**3**), which was identified by a single-crystal structure analysis. For **3**, $a = 15.554$ (5) Å, $b = 9.246$ (4) Å, $c = 22.952)$ Å, $\beta = 101.98$ (4)°, space group $P2_1/c$, $Z = 4$, $R = 0.061$, and $R_w = 0.092$. The geometry of **3** is similar to that observed for **2d** and **2j** with silyl ligands trans to P and hydride trans to CO.

Introduction

The oxidative addition of silanes to complexes of the platinum group elements has been well documented.[1-3] Many of these examples include the addition of silanes to d^8 Ir(I) complexes generating iridium(III) silyl hydride products.[4-12] A few, less common examples involve reaction of silanes with Ir(III) complexes, which, for the most part, proceed by prior reductive elimination to Ir(I). The iridium(III) silyl hydride complexes generated in these reactions often undergo secondary chemistry through reductive elimination and subsequent oxidative addition, leading to ligand redistribution and the formation of alkylsilyl halides, disilanes, or disiloxanes.[7,14,15] Iridium(III) silyl complexes have recently been used to synthesize alkoxysilanes,[12] and redistribution of the groups bound to silicon in the presence of iridium(I) complexes has been observed.[16]

Silyl hydride complexes have also been observed to promote silicon-carbon bond formation in hydrosilation catalysis and in dehydrogenative silylation as in eq 1.[17] The latter may occur via olefin insertion into the M-Si bond, a process that has only recently been documented.[18]

$$C_2H_4 \xrightarrow{IrH_2(SiEt_3)(cod)(PPh_3)} CH_2{=}CHSiEt_3 + SiEt_4 \qquad (1)$$

In this paper we report the synthesis and characterization of a series of mono- and bis(silyl) complexes of general formulas $IrH_2(SiR_nH_{3-n})(CO)(dppe)$ and $IrH(SiR_nH_{3-n})_2(CO)(dppe)$, which are prepared from the reaction of primary and secondary silanes with the Ir(III) trihydride complex $IrH_3(CO)(dppe)$ (dppe = 1,2-bis(diphenylphosphino)ethane).[19] This work was undertaken as part of a continuing series of studies on oxidative-addition reactions and related chemistry of iridium dppe complexes.[15,19]

Results and Discussion

Mono(silyl) Complexes. The trihydride complex $IrH_3(CO)(dppe)$, which has been characterized previously,[19] reacts cleanly with primary, secondary, and tertiary silanes to produce the iridium(III) silyl dihydride complexes $IrH_2(SiR_nH_{3-n})(CO)(dppe)$ (**1a–i**). The formation of **1b** has previously been reported as a secondary product in the reaction of IrBr(CO)dppe with Et_3SiH.[15] Analogues of these complexes having the general formulas $[IrH_2(SiR_nH_{3-n})(CO)(PPh_3)_2]$ are known in which two PPh_3 ligands are present in place of dppe.[5b,6b,7,10,20]

These silylbis(hydrido)iridium complexes are colorless and stable in air as solids. Their characterization was performed by ^1H and ^{31}P NMR and IR spectroscopies. The M-H resonances and the proton-phosphorus coupling constants enable one to assign the position of the hydride ligands relative to the chelating dppe bis(phosphine) ligand. One hydride resonance is a pseudotriplet with $J_{P-H} = 16-22$ Hz, which is typical for a hydride cis to two nearly equivalent phosphorus atoms,[21] while the other hydride

---

(1) MacKay, K. M.; Nicholson, B. K. In *Comprehensive Organometallics*; Wilkinson, G., Stone, F. G. A., Abel, E. W., Eds.; Pergamon: Oxford, England, 1982; Vol. 6, Chapter 43, p 1043.

(2) *The Chemistry of Organic Silicon Compounds*; Patai, S., Rappoport, Z., Eds.; John Wiley & Sons: New York, 1989; Part 2, Chapter 24, p 1417.

(3) Aylett, B. J. *Adv. Inorg. Chem. Radiochem.* **1982**, *25*, 1.

(4) Harrod, J. F.; Smith, C. A.; Than, K. A. *J. Am. Chem. Soc.* **1972**, *94*, 8321-5.

(5) (a) Fawcett, J. P.; Harrod, J. F. *J. Organomet. Chem.* **1976**, *113*, 245-8. (b) Fawcett, J. P.; Harrod, J. F. *Can. J. Chem.* **1976**, *54*, 3102-9. (c) Harrod, J. F.; Gilson, D. F. R.; Charles, R. *Can. J. Chem.* **1968**, *47*, 2205.

(6) (a) Chalk, A. J.; Harrod, J. F. *J. Am. Chem. Soc.* **1965**, *87*, 16-21. (b) Chalk, A. J. *J. Chem. Soc., Chem. Commun.* **1969**, 1207-8.

(7) Bennett, M. A.; Charles, R.; Fraser, P. J. *Aust. J. Chem.* **1977**, *30*, 1201-11.

(8) (a) Blackburn, S. N.; Hazeldine, R. N.; Parish, R. N.; Parish, R. V.; Setchfield, J. H. *J. Chem. Res., Synop.* **1980**, 170-7. (b) Hazeldine, R. N.; Parish, R. V.; Setchfield, J. H. *J. Organomet. Chem.* **1973**, *57*, 279-85. (c) Blackburn, S. N.; Hazeldine, R. N.; Parish, R. V.; Setchfield, J. H. *Ibid.* **1980**, *192*, 329-38.

(9) (a) Ebsworth, E. A. V.; Fraser, T. E.; Henderson, S. G.; Leitch, D. M.; Rankin, D. W. H. *J. Chem. Soc., Dalton Trans.* **1981**, 1010-8. (b) Ebsworth, E. A. V.; Fraser, T. E. *Ibid.* **1979**, 1960-4. (c) Ebsworth, E. A. V.; Leitch, D. M. *Ibid.* **1973**, 1287-92.

(10) Glockling, F.; Irwin, J. G. *Inorg. Chim. Acta* **1972**, *6*, 355-8.

(11) Auburn, M. J.; Stobart, S. R. *J. Chem. Soc., Chem. Commun.* **1984**, 281-2.

(12) (a) Rappoli, B. J.; Janik, T. S.; Churchill, M. R.; Thompson, J. S.; Atwood, J. D. *Organometallics* **1988**, *7*, 1939-44. (b) Crabtree, R. H.; Luo, X.-L. *J. Am. Chem. Soc.* **1987**, *6*, 1590.

(13) (a) Fernandez, M.-J.; Maitlis, P. M. *Organometallics* **1983**, *2*, 164. (b) Fernandez, M.-J.; Maitlis, P. M. *J. Chem. Soc., Dalton Trans.* **1984**, 2063.

(14) Brown-Wensley, K. A. *Organometallics* **1987**, *6*, 1590.

(15) Johnson, C. E.; Eisenberg, R. *J. Am. Chem. Soc.* **1985**, *107*, 6531.

(16) Curtis, M. D.; Epstein, P. S. *Adv. Organomet. Chem.* **1981**, *19*, 213.

(17) Fernandez, M.-J.; Esteruelas, M. A.; Jimenez, M. S.; Oro, L. A. *Organometallics* **1986**, *5*, 1519.

(18) Randolph, C. L.; Wrighton, M. S. *J. Am. Chem. Soc.* **1986**, *108*, 3366-74.

(19) (a) Fisher, B. J.; Eisenberg, R. *Organometallics* **1983**, *2*, 764. (b) Deutsch, P. P.; Eisenberg, R. *J. Am. Chem. Soc.* **1990**, *112*, 714 and references therein.

(20) Harrod, J. F.; Gilson, D. F. R.; Charles, R. *Can. J. Chem.* **1968**, *47*, 2205.

displays a doublet of doublets pattern with one large trans phosphorus coupling (J_{H-P} = 100–126 Hz) and one cis phosphorus coupling (J_{H-P} = 9–14 Hz). The ^{1}H NMR data for these complexes are presented in Table I.

The IR data for complexes **1a–i** (see Table I) provide additional information regarding the coordination geometry, allowing its unequivocal assignment for these systems. Specifically, the carbonyl stretch ν_{CO} is lower than that expected for carbonyl bound to Ir(III), while one of the Ir–H stretches is of significantly higher energy and intensity than expected. For the complex $IrH_2(Me_3Si)(CO)(dppe)$ (**1c**) for example, ν_{CO} appears at 1958 cm^{-1}, while ν_{MH} is seen at 2073 and 2020 cm^{-1} with the former having higher intensity. The shifts in ν_{CO} and ν_{MH} from expected values and intensities can be attributed to coupling between CO and MH oscillators when a hydride ligand occupies a position trans to a carbonyl.[22] This type of coupling has been observed previously. Thus, from the ^{1}H NMR and IR data, the coordination geometry of the $IrH_2(SiR_nH_{3-n})(CO)(dppe)$ complexes can be assigned unambiguously with cis phosphines and cis hydrides, one of which is trans to a carbonyl.

The reaction of $IrH_3(CO)(dppe)$ with silanes occurs rapidly at 60° C in C_6D_6 and initiates with loss of H_2 as in eq 2. Molecular hydrogen is seen in the ^{1}H NMR spectrum of the reaction mixture,[23] and while the four-coordinate species A is not observed directly, its existence seems highly probable. This coordinatively unsaturated species has been postulated in other reports as an intermediate in related exchange reactions proceeding by reductive elimination and oxidative addition or ligand coordination.[15,19,22b,24] The subsequent oxidative addition of alkyl silanes leading to **1a–i** in eq 2 occurs readily, being fastest for silanes containing electronegative substituents.

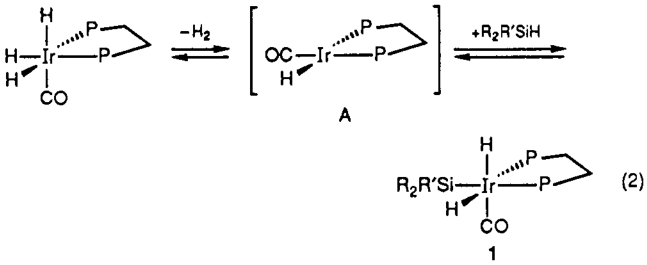

The fact that reductive elimination and oxidative addition of silane is facile and rapid is evidenced by exchange of the silyl ligand when the solution is heated in the presence of a more reactive silane. For example, when $IrH_2(Me_3Si)(CO)(dppe)$ (**1c**) is heated in C_6D_6 at 60 °C for 10 min with Me_2SiH_2, free Me_3SiH and $IrH_2(Me_2SiH)(CO)(dppe)$ (**1g**), are observed in the ^{1}H NMR spectrum of the reaction solution.

Investigation of the possibility of H_2 loss from the mono(silyl) complexes was carried out by placing a C_6D_6 solution of $IrH_2(Et_3Si)(CO)(dppe)$ (**1b**) under 300 Torr of D_2 and heating the solution at 60 °C for 24 h. The ^{1}H NMR spectrum of the reaction solution revealed that 75% conversion to the dideuteride had occurred, as indicated by a decrease in the integrated intensities of the hydride resonances relative to the dppe and silyl resonances.

Reactions of $IrH_2(SiR_3)(CO)(dppe)$ (R = Me, Et) with C_2H_4. The dihydrido silyl complexes formed with Et_3SiH and Me_3SiH (**1b,c**, respectively) react with C_2H_4 to afford the products of ethylene hydrosilation, hydrogenation, and dehydrogenative silylation. The organosilicon products from these reactions were identified by ^{1}H NMR spectroscopy and in the case of **1c** were confirmed by GC/MS.[25] Oro and co-workers[17] have previously reported a related iridium system that promotes the unusual dehydrogenative silylation reaction competitive with hydrogenation and hydrosilation. The reaction of $IrH_2(Me_3Si)(CO)(dppe)$ (**1c**) with ethylene at 60 °C in C_6D_6, shown in eq 3, yields the hydrosilated and dehydrogenatively silated products in a 3:1 ratio.

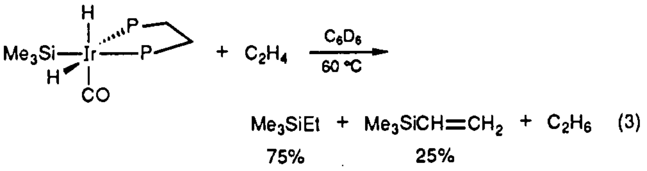

The appearance of the unsaturated organosilane product $Me_3SiCH{=}CH_2$ raises an interesting mechanistic question. In the Chalk–Harrod mechanism of hydrosilation, the olefin inserts into the metal–hydrogen bond to yield an alkylsilyl intermediate followed by reductive elimination of the alkylsilane. The stoichiometric steps involved in this mechanism, including the elimination step are known.[26] However, there is now evidence for an alternative possibility in which the olefin inserts into the metal–silicon bond to generate a β-silylalkyl hydride intermediate. This insertion was suggested by Ojima in 1984[27] and then demonstrated by Randolph and Wrighton,[18] who isolated the β-silylalkyl complex $(\eta^5\text{-}C_5Me_5)Fe(CO)L(CH_2CH_2SiMe_3)$. This complex was generated by the photolysis of $(\eta^5\text{-}C_5Me_5)Fe(CO)_2(SiMe_3)$ in the presence of ethylene followed by addition of ligand L (CO, PPh_3).[18] In the absence of ligand, the β-silylalkyl complex was found to undergo β-hydrogen elimination to yield the vinylsilane.[18] Very recently, additional evidence for olefin insertion into M–Si has been provided by the structural characterization of an ethylene insertion product into a Zr–Si bond.[28]

While slow consumption of ethylene in the reactions with $IrH_2(Et_3Si)(CO)(dppe)$ (**1b**) and $IrH_2(Me_3Si)(CO)(dppe)$ (**1c**) was observed for several days, decomposition of the triethylsilyl complex **1b** was noted after this time. For the trimethylsilyl system (**1c**), reaction continued until the appearance of resonances consistent with the formation of a bis(silyl) complex in the reaction solution (vide infra).

Bis(silyl) Complexes. The silyl dihydride complexes **1c–i** react further with excess silane to produce the hydrido bis(silyl) complexes **2c–i**. The NMR and IR data for these complexes are presented in Table II. These bis(silyl) complexes undoubtedly form by reductive elimination of H_2 from **1c–i** followed by oxidative addition of a second molecule of silane, as shown in eq 4.

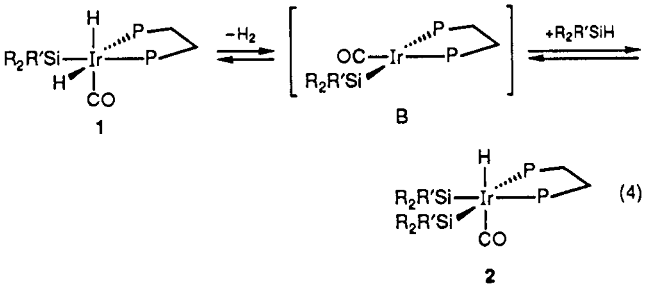

In support of this mechanism, H_2 is observed in the ^{1}H NMR spectrum of the reaction solutions,[23] although the four-coordinate intermediates B are not. However, the latter is not surprising in light of the elusiveness of the coordinatively unsaturated Ir(I) intermediate $IrH(CO)(dppe)$ (A) in oxidative-addition/reductive-elimination sequences.

---

(21) Crabtree, R. H.; Felkin, H.; Fillebeen-Khan, T.; Morris, G. E. *J. Organomet. Chem.* **1979**, *168*, 183.

(22) (a) Vaska, L. *J. Am. Chem. Soc.* **1966**, *88*, 4100. (b) Coupling of the Ir–H and Ir–CO oscillators is shown by the following comparison: ν_{CO} for $IrH_3(CO)(dppe)$ is 1960 cm^{-1}, while ν_{CO} is 2030 cm^{-1} for $IrD_3(CO)(dppe)$. Johnson, C. E.; Eisenberg, R. *J. Am. Chem. Soc.* **1985**, *107*, 3148.

(23) H_2 in C_6D_6 appears as a singlet at 4.46 ppm in the ^{1}H NMR spectrum.

(24) Johnson, C. E.; Fisher, B. J.; Eisenberg, R. *J. Am. Chem. Soc.* **1983**, *105*, 7772.

(25) ^{1}H NMR (C_6D_6) and MS data are as follows. Me_3SiEt: δ 6.17 (m, 1 H), 5.90 (m, 1 H), 5.65 (m, 1 H), 0.04 (s, 9 H); *m/e* = 102. $Me_3Si(C_2H_3)$: δ 0.94 (t, 3 H), 0.45 (q, 2 H), 0.01 (s, 9 H); *m/e* = 100.

(26) Blakeney, A. J.; Gladyz, J. A. *Inorg. Chim. Acta* **1981**, *53*, L25.

(27) Ojima, I.; Fuchikami, T.; Yatabe, M. *J. Organomet. Chem.* **1984**, *260*, 335–46.

(28) Arnold, J.; Engeler, M. P.; Elsner, F. H.; Heyn, R. H.; Tilley, T. D. *Organometallics* **1989**, *8*, 2284–6.

(29) (a) Kiso, Y.; Tamao, K.; Kumada, M. *J. Organomet. Chem.* **1974**, *76*, 95. (b) Haszeldine, R. N.; Parish, R. V.; Parry, D. J. *J. Chem. Soc. A* **1969**, 683.

Table I. ^1H and ^{31}P NMR and IR Data for the Mono(silyl) Dihydride Complexes $IrH_2(SiR_nH_{3-n})(CO)(dppe)$

compd	δ_{Ir-H} (J_{P-H}, Hz)	δ_{CH}(dppe)	$\delta_{Ph\ o-H}$(dppe)	δ_{R_nSi}	$\delta_{H_{3-n}Si}$	δ_P	ν_{Si-H}, cm^{-1}	ν_{Ir-H}, cm^{-1}	ν_{CO}, cm^{-1}
$IrH_2(Ph_3Si)(CO)(dppe)$ (**1a**)	−9.43 (dd, 10.7, 116.1, −10.20 (t, 19.2)	2.25–1.80 (m, 4 H)	7.91 (m), 7.61 (m), 7.43 (m)	7.92 (m) (Ph *o*-H)				2122	1972
$IrH_2(Et_3Si)(CO)(dppe)$ (**1b**)	−10.06 (dd, 10.6, 117.5), −10.69 (t, 19.6)	2.18 (m, 1 H), 1.99 (m, 2 H), 1.78 (m, 1 H)	7.90 (m, 2 H), 7.64 (m, 2 H), 7.51 (m, 2 H), 7.47 (m, 2 H)	1.32 (t, 9 H), 1.12 (m, 6 H)				2070	1957
$IrH_2(Me_3Si)(CO)(dppe)$ (**1c**)	−9.67 (dd, 11.0, 117.0), −10.34 (t, 18.3)	2.21 (m, 1 H), 2.21 (m, 2 H), 1.82 (m, 1 H)	7.86 (m, 2 H), 7.64 (m, 2 H), 7.56 (m, 2 H), 7.47 (m, 2 H)	0.87 (s, 9 H)		28.9 26.1		2073, 2020	1958
$IrH_2(Me_2ClSi)(CO)(dppe)$ (**1d**)	−9.91 (dd, 13.7, 114.4), −10.41 (t, 19.8)	2.22 (m, 1 H), 1.92 (m, 3 H)	7.80 (m, 4 H), 7.53 (m, 2 H), 7.36 (m, 2 H)	1.32 (s, 3 H), 0.94 (s, 3 H)				2076, 2032	1961
$IrH_2(MeCl_2Si)(CO)(dppe)$ (**1e**)	−9.71 (dd, 13.0, 115.0), −10.34 (t, 20.0)	2.20–1.75 (m, 4 H)	7.82 (m, 2 H), 7.73 (m, 2 H), 7.52 (m, 2 H), 7.28 (m, 2 H)	1.50 (s, 3 H)				2093, 2030	1989
$IrH_2(Ph_2HSi)(CO)(dppe)$ (**1f**)	−9.28 (ddd, 9.75, 102.5) (J_{H-H} = 2.4 Hz)	2.14 (m, 2 H), 1.88 (m, 2 H)	7.85 (m, 2 H), 7.45 (m, 2 H), 7.28 (t, 2 H), 7.22 (t, 2 H)	8.27 (d, 2 H), 7.98 (d, 2 H)	6.04 (m, 1 H)		2134	2099	1976
$IrH_2(Me_2HSi)(CO)(dppe)^b$ (**1g**)	−9.60 (dd, 11.0, 126.0), −10.42 (t, 19.5)	2.03 (m, 2 H), 1.80 (m, 2 H)	7.36 (m), 7.65 (m), 7.48 (m)	1.06 (m, 6 H)	5.26 (m, 1 H)			2074, 2039	1959
$IrH_2(PhH_2Si)(CO)(dppe)^a$ (**1h**)	−9.45 (dd, 11.0, 138.0), −10.54 (t, 19.5)	2.15 (m, 2 H), 1.86 (m, 2 H)	7.81 (m, 2 H), 7.58 (m, 4 H), 7.39 (m, 2 H)	8.17 (d, 2 H) (Ph *o*-H)	5.39 (m, 2 H)		2170	2078, 2041	1970
$IrH_2(EtH_2Si)(CO)(dppe)^b$ (**1i**)	−9.67 (dd, 11.6, 117.6), −10.66 (t, 16.9)	2.03 (m, 2 H), 1.78 (m, 2 H)	7.83 (m, 2 H), 7.62 (m, 4 H), 7.49 (m, 2 H)		4.73 (m, 1 H), 4.64 (m, 1 H)		2153	2076, 2035	1964

[a] Phenyl *o*-H proton assignments are not unambiguous. [b] Due to overlap of resonances from mono- and bis(silyl) complexes, explicit determination of chemical shift and/or integral was not possible.

Table II. ^1H and ^{31}P NMR and IR Data for the Bis(silyl) Hydride Complexes $IrH(SiR_nH_{3-n})_2(CO)(dppe)$ and $IrH(EtF_2Si)_2(CO)(dppe)$

compd	δ_{Ir-H} (J_{P-H}, Hz)	δ_{CH}(dppe)	$\delta_{Ph\ o-H}$(dppe)	δ_{R_nSi}	$\delta_{H_{3-n}Si}$	δ_P	ν_{Si-H}, cm^{-1}	ν_{Ir-H}, cm^{-1}	ν_{CO}, cm^{-1}
$IrH(Me_3Si)_2(CO)(dppe)$ (**2c**)	−9.72 (t, 17.5)	1.76 (m, 2 H), 1.71 (m, 2 H)	7.73 (m, 8 H)	0.69 (s, 18 H)		27.7		2065	1951
$IrH(Me_2ClSi)_2(CO)(dppe)$ (**2d**)	−9.56 (t, 18.3)	1.72 (m, 2 H), 1.67 (m, 2 H)	7.73 (m, 8 H)	1.08 (s, 6 H), 0.80 (s, 6 H)		27.4		2084	1973
$IrH(MeCl_2Si)_2(CO)(dppe)$ (**2e**)	−9.48 (t, 16.8)	1.69–1.63 (m, 4 H)	7.68 (m, 8 H)	1.33 (s, 6 H)				2106	1999
$IrH(Ph_2HSi)_2(CO)(dppe)$ (**2f**)	−9.59 (t, 17.1)	2.10 (m, 2 H), 1.88 (m, 2 H)	7.85 (m), 7.48 (m), 7.31 (m)	7.64 (m), 7.49 (m) (Ph *o*-H)	6.14 (dd, 2 H)	25.6	2097	2069	1974
$IrH(Me_2HSi)_2(CO)(dppe)$ (**2g**)	−10.05 (t, 16.0)	1.98 (m, 2 H), 1.77 (m, 2 H)	7.63 (t, 4 H), 7.56 (t, 4 H)	0.84 (m, 6 H), 0.80 (m, 6 H)	4.96 (m, 2 H)	28.7	2080	2022	1965
$IrH(PhH_2Si)_2(CO)(dppe)^a$ (**2h**)	−10.35 (t, 18.2)	2.08 (m, 2 H), 1.76 (m, 2 H)	7.55 (m, 4 H), 7.32 (m, 4 H)	7.62 (m, 4 H) (Ph *o*-H)	5.22 (m, 2 H), 5.11 (m, 2 H)			2084	1973
$IrH(EtH_2Si)_2(CO)(dppe)$ (**2i**)	−10.51 (t, 17.1)	2.08 (m, 2 H), 1.76 (m, 2 H)	7.62 (t, 4 H), 7.53 (m, 4 H)	1.33 (t, 6 H), 1.17 (m, 4 H)	4.39 (m, 4 H)	28.7	2112	2064	1971
$IrH(Me_2HSi)(Me_2ClSi)(CO)(dppe)$ (**2j**)	−9.87 (t, 18.2)	2.26–1.43 (m)	7.88, 7.72, 7.14, 7.06, 7.40 (m's)	1.21 (s), 0.86 (m), 0.81 (m), 0.65 (m)	4.99, 4.67 (m's)	28.7	2031	1995	1958
$IrH(EtF_2Si)_2(CO)(dppe)$ (**3**)	−9.93 (m)	1.79, 1.53 (m's, 4 H)	7.43 (m, 8 H)	0.90 (m, 6 H), 0.81 (m, 4 H)		26.7		2129	1986

[a] Phenyl *o*-H proton assignments are not unambiguous. [b] Due to overlap of resonances from mono- and bis(silyl) complexes, explicit determination of chemical shift and/or integral was not possible.

Table III. Selected Crystal Data, Data Collection, and Structure Refinement Parameters[a]

	2d	**2j**	**3**
formula	$IrCl_2P_2Si_2OC_{31}H_{37}$	$IrClP_2Si_2OC_{31}H_{38}$	$IrP_2Si_2F_4OC_{31}H_{35}$
fw	806.88	769.41	809.95
space group	$P\bar{1}$ (No. 2)	$P\bar{1}$ (No. 2)	$P2_1/c$ (No. 14)
a, Å	12.952 (2)	11.976 (5)	15.554 (5)
b, Å	15.480 (5)	15.816 (9)	9.246 (4)
c, Å	9.567 (2)	9.357 (3)	22.95 (2)
α, deg	100.58 (2)	93.43 (4)	90.00
β, deg	111.55 (1)	110.01 (3)	101.98 (4)
γ, deg	105.73 (2)	77.59 (4)	90.00
V, Å^3	1629 (2)	1626 (3)	3229 (6)
Z	2	2	4
d_{calcd}, g/cm^3	1.64	1.57	1.67
abs coeff, (μ(Mo Kα)), cm^{-1}	47.02	46.28	43.37
transm coeff	0.77–1.04	0.89–1.04	0.65–1.73
$R(F_o)$	0.029	0.035	0.061
$R_w(F_o)$	0.041	0.046	0.092

[a] For the three structure determinations, data were measured at 23 °C by using Mo Kα radiation, $\lambda = 0.71069$ Å.

Assignment of the coordination geometry of **2c–i** is straightforward on the basis of the NMR and IR spectroscopic data given in Table II. The iridium-hydride resonance in all cases is a triplet with $J_{H-P} = 16-18$ Hz, indicating a hydride cis to two equivalent phosphorus atoms.[21] The $^{31}P\{^1H\}$ NMR spectra of the complexes consist of a singlet, indicative of equivalent phosphines. Thus, both phosphines must have the same trans ligand, which for **2c–i** are the silyl groups. Finally, as in the case of the mono(silyl) complexes, the lower ν_{CO} for carbonyl bound to Ir(III) indicates a geometry that places the hydride ligand trans to the carbonyl ligand.[22]

The mono(silyl) complexes $IrH_2(Ph_3Si)(CO)(dppe)$ (**1a**) and $IrH_2(Et_3Si)(CO)(dppe)$ (**1b**) do not form bis(silyl) systems, possibly because of steric factors. For the trimethylsilyl system **1c**, it appears that ethylene is required for formation of the analogous bis(silyl) complex. The role of ethylene in this reaction may be simply that of a hydrogen sink through the formation of ethane. Removal of H_2 via hydrogenation eliminates a potentially more reactive substrate, molecular hydrogen, from reacting with B. The reaction of the mono(silyl) complexes **1c–i** with a second mole of silane to yield the respective bis(silyl) complexes **2c–i** occurs at different rates and is observed to be slowest for the trimethylsilyl system (the conversion of **1c** to **2c**). The recently reported complex $Ir(Et)(CH_2{=}CH_2)(CO)(dppe)$[30a] also reacts with excess Me_3SiH to yield **2c**, and the bis(silyl) product is formed more rapidly than when **1c** is used as the starting material.[30b] The faster reaction rate may be due to the fact that $Ir(Et)(CH_2{=}CH_2)(CO)(dppe)$ contains a hydrogen sink (ethylene) within its coordination sphere. It thus may be possible to prepare the bis(silyl) complexes of triphenyl- and triethylsilane by using $Ir(Et)(CH_2{=}CH_2)(CO)(dppe)$.

Both $IrH(Me_3Si)_2(CO)(dppe)$ (**2c**) and $IrH(Me_2ClSi)_2(CO)(dppe)$ (**2d**) display dppe methylene resonances, which appear to show equivalence of the $-CH_2-$ protons similar to that found for $IrH(CO)_2(dppe)$,[31] a five-coordinate, fluxional complex of Ir(I). In order to probe the possibility of fluxionality or of an equilibrium involving a coordinatively unsaturated species, a C_6D_6 solution of **2d** was placed under 500 Torr of ^{13}CO. Incorporation of ^{13}CO into **2d** was not observed, thereby ruling against dissociation of ligand and subsequent exchange to explain the observed methylene resonances. Moreover, **2c** and **2d** do not appear to be stereochemically nonrigid on the basis of the fact that the Ir–H triplet remains sharp in ^1H NMR spectra down to −77 °C. This result agrees with that found for the other bis(silyl) complexes, which exhibit resonances for the methylene protons consistent with a static octahedral structure. Therefore, the apparant equivalence of the dppe $-CH_2-$ protons in **2c** and **2d** appears to be an artifact.

The reaction of $IrH_3(CO)(dppe)$ with Me_2SiH_2 yielded a complex ^1H NMR spectrum that indicated an approximately 50:50 mixture of two iridium hydride complexes and minor amounts of others. While one set of the predominant resonances (Ir–H, Si–H, Si–CH_3) corresponded to the expected product $IrH(Me_2SiH)_2(CO)(dppe)$ (**2g**), the other set was not assigned until an X-ray diffraction study revealed the presence of the mixed bis(silyl) complex $IrH(Me_2SiH)(Me_2SiCl)(CO)(dppe)$ (**2j**). The minor hydride products have not been identified but may include a binuclear species with μ-$SiMe_2$ groups.

Molecular Structures of the Bis(silyl) Complexes. The molecular structures of the bis(silyl) complexes $IrH(SiClMe_2)_2(CO)(dppe)$ (**2d**) and $IrH(Me_2SiH)(Me_2SiCl)(CO)(dppe)$ (**2j**) were determined by single-crystal X-ray studies. Table III is an abbreviated presentation of the crystal data and structure refinement parameters for the structure determinations (Table SI in the supplementary material gives a full tabulation). In accord with the assignment based on spectroscopy, complex **2d** possesses an octahedral coordination geometry with equivalent $ClMe_2Si-$ ligands trans to the phosphine donors of the dppe ligand. Although the hydride was not located in the structure determination, it is clear that the hydride and carbonyl ligands occupy the remaining positions, which are mutually trans. A perspective drawing of the complex is shown in Figure 1. Table IV contains the refined positional and isotropic thermal parameters for the structure, while Tables V and VI contain selected bond distances and angles for **2d**.

The Ir–Si distance of 2.396 (2) Å in **2d** is slightly but significantly shorter than the 2.414-Å value in $IrH_2(SiMe_2Ph)(P(p\text{-}tol)_3)_2$[32] and the distance of 2.418 Å for Ir–$SiHMe_2$ discussed below. This difference may be attributable to the chloro substituent on the silyl group, which not only imparts greater reactivity for $ClMe_2SiH$ relative to Me_2SiH_2 but also makes the Ir–Si bond of the former slightly stronger. Support for this view is also obtained from the Ir–P and Ir–CO bond distances (2.368 (2) and 1.93 (1) Å, respectively), which are slightly longer in the structure of **2d** relative to those in the closely related system $IrH_2Br(CO)(dppe)$ (2.334 (3) and 1.84 (1) Å).[33]

The complex $IrH(Me_2SiH)(Me_2SiCl)(CO)(dppe)$ (**2j**) was identified from its crystal structure determination as a mixed bis(silyl) complex in which both dimethylsilyl and chlorodimethylsilyl groups are coordinated to iridium. Figure 2 shows a perspective drawing of the complex **2j**. Table VII contains the refined positional and isotropic thermal parameters for the structure, while Tables VIII and IX contain selected bond distances and angles for **2j**. The geometry is essentially the same as that found for **2d**.

The most curious aspect of the structure is the existence of the chlorodimethylsilyl ligand in a product arising from a reaction in which no chloride was thought to be present. In retrospect,

---

[30] Deutsch, P. P.; Eisenberg, R. Unpublished results.

[31] Vaska, L.; Catone, D. L. *J. Am. Chem. Soc.* **1966**, *88*, 5324.

[32] Rappoli, B. J.; Janik, T. S.; Churchill, M. R.; Thompson, J. S.; Atwood, J. D. *Organometallics* **1988**, *7*, 1939–44.

[33] Johnson, C. E.; Eisenberg, R. *Organometallics* **1985**, *107*, 3148.

Table IV. Refined Positional and Isotropic Thermal Parameters and Their Estimated Standard Deviations for $IrH(SiHMe_2)(SiClMe_2)(CO)(dppe)$ (**2d**)

atom	*x*	*y*	*z*	*B*(eq), Å^2
Ir	0.27471 (3)	0.22040 (2)	−0.00368 (3)	2.68 (1)
Cl1	0.0126 (2)	0.2658 (2)	−0.2625 (3)	5.4 (1)
Cl2	0.4037 (3)	0.1808 (2)	−0.2947 (3)	6.0 (1)
Cl3	0.531 (1)	0.148 (1)	0.014 (2)	3.3 (4)
P1	0.3872 (2)	0.2173 (2)	0.2530 (3)	2.88 (7)
P2	0.2337 (2)	0.3387 (1)	0.1376 (3)	2.81 (7)
Si1	0.1695 (2)	0.2422 (2)	−0.2511 (3)	3.30 (8)
Si2	0.3626 (2)	0.1318 (2)	−0.1243 (3)	3.40 (8)
O	0.0713 (6)	0.0327 (5)	−0.1071 (8)	5.4 (3)
C1	0.1439 (8)	0.1033 (7)	−0.066 (1)	3.6 (3)
C2	0.3511 (7)	0.2897 (6)	0.3906 (9)	3.2 (3)
C3	0.3481 (7)	0.3773 (6)	0.344 (1)	3.4 (3)
C4	0.2496 (9)	0.3483 (7)	−0.291 (1)	4.4 (3)
C5	0.0967 (8)	0.1374 (7)	−0.438 (1)	4.8 (3)
C6	0.511 (1)	0.121 (1)	0.011 (2)	3.5 (4)
C7	0.271 (1)	0.0015 (6)	−0.233 (1)	5.3 (4)
C11	0.3515 (7)	0.1025 (5)	0.2829 (9)	2.7 (3)
C12	0.4248 (8)	0.0519 (7)	0.297 (1)	4.4 (4)
C13	0.390 (1)	−0.0378 (7)	0.314 (1)	5.5 (4)
C14	0.284 (1)	−0.0742 (7)	0.319 (1)	5.5 (4)
C15	0.2100 (9)	−0.0250 (7)	0.303 (1)	4.6 (4)
C16	0.2422 (8)	0.0605 (6)	0.283 (1)	3.8 (3)
C21	0.5498 (7)	0.2761 (6)	0.355 (1)	3.1 (3)
C22	0.6100 (8)	0.3382 (6)	0.298 (1)	3.9 (3)
C23	0.7318 (9)	0.3868 (6)	0.383 (1)	4.7 (4)
C24	0.7941 (8)	0.3746 (7)	0.522 (1)	4.4 (3)
C25	0.7359 (9)	0.3162 (7)	0.580 (1)	4.5 (3)
C26	0.6149 (8)	0.2672 (6)	0.500 (1)	4.0 (3)
C31	0.0971 (7)	0.3084 (6)	0.167 (1)	3.2 (3)
C32	0.0872 (8)	0.3694 (6)	0.282 (1)	3.9 (3)
C33	−0.006 (1)	0.3463 (8)	0.315 (1)	4.8 (4)
C34	−0.098 (1)	0.2592 (8)	0.231 (1)	5.1 (4)
C35	−0.0930 (8)	0.1994 (7)	0.113 (1)	5.4 (4)
C36	0.0040 (8)	0.2229 (6)	0.080 (1)	4.4 (3)
C41	0.2510 (8)	0.4492 (6)	0.093 (1)	3.3 (3)
C42	0.3641 (9)	0.5055 (7)	0.114 (1)	4.8 (4)
C43	0.380 (1)	0.5890 (7)	0.079 (1)	6.0 (4)
C44	0.288 (1)	0.6178 (7)	0.023 (1)	6.2 (5)
C45	0.179 (1)	0.5644 (8)	0.000 (1)	6.0 (5)
C46	0.1581 (9)	0.4783 (7)	0.034 (1)	4.7 (4)

Table V. Selected Intramolecular Distances (Å) for $IrH(SiClMe_2)_2(CO)(dppe)$ (**2d**)[a]

Ir–C1	1.93 (1)	P1–C2	1.845 (8)
Ir–P1	2.368 (2)	P2–C41	1.816 (8)
Ir–P2	2.369 (2)	P2–C31	1.840 (8)
Ir–Si2	2.396 (2)	P2–C3	1.844 (8)
Ir–Si1	2.397 (2)	Si1–C4	1.87 (1)
Cl1–Si1	2.128 (3)	Si1–C5	1.90 (1)
Cl2–Si2	2.094 (3)	Si2–C7	1.89 (1)
Cl3–C6	0.42 (2)	Si2–C6	1.95 (1)
Cl3–Si2	2.01 (1)	O–C1	1.12 (1)
P1–C11	1.815 (8)	C2–C3	1.51 (1)
P1–C21	1.827 (8)		

[a] Estimated standard deviations in the least significant figure are given in parentheses.

Table VI. Selected Bond Angles (deg) for $IrH(SiClMe_2)_2(CO)(dppe)$ (**2d**)[a]

C1–Ir–P1	96.2 (3)	C41–P2–C3	102.5 (4)
C1–Ir–P2	106.1 (3)	C41–P2–Ir	119.1 (3)
C1–Ir–Si2	87.9 (3)	C3–P2–Ir	105.5 (3)
C1–Ir–Si1	89.1 (3)	C4–Si1–C5	108.2 (4)
P1–Ir–P2	83.15 (7)	C4–Si1–Cl1	102.3 (3)
P1–Ir–Si2	93.58 (8)	C4–Si1–Ir	116.4 (3)
P1–Ir–Si1	173.66 (7)	C5–Si1–Cl1	98.1 (3)
P2–Ir–Si2	165.83 (7)	C5–Si1–Ir	118.3 (3)
P2–Ir–Si1	92.07 (8)	Cl1–Si1–Ir	110.8 (1)
Si2–Ir–Si1	90.06 (8)	C6–Si2–Cl2	103.1 (4)
C11–P1–C21	106.9 (4)	C6–Si2–Ir	118.6 (4)
C11–P1–C2	104.5 (4)	C7–Si2–C6	98.6 (6)
C11–P1–Ir	115.9 (3)	C7–Si2–Cl2	103.0 (3)
C21–P1–C2	98.1 (4)	C7–Si2–Ir	116.8 (3)
C21–P1–Ir	121.7 (3)	Cl2–Si2–Ir	114.3 (1)
C2–P1–Ir	106.9 (3)	O–C1–Ir	175.5 (8)
C31–P2–C3	100.3 (4)	C3–C2–P1	107.7 (5)
C31–P2–Ir	120.7 (3)	C2–C3–P2	107.5 (6)
C41–P2–C31	105.6 (4)		

[a] Estimated standard deviations in the least significant figure are given in parentheses.

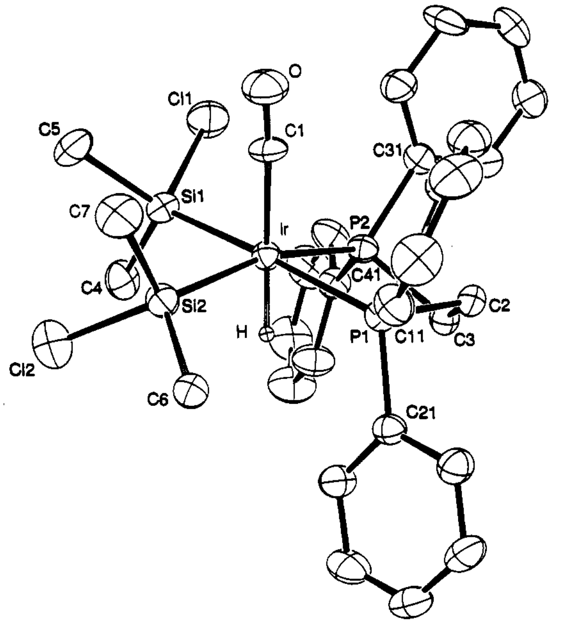

Figure 1. Perspective drawing of the coordination geometry of **2d**. The hydride ligand was not located in the actual structure determination. The phenyl carbon atoms are numbered sequentially with the ipso carbon being C*n*1 and the para carbon being C*n*4.

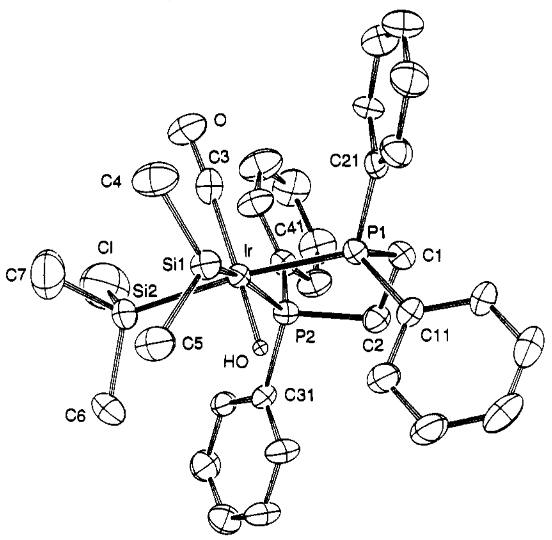

Figure 2. Perspective drawing of the coordination geometry of **2j**. The phenyl carbon atoms are numbered sequentially with the ipso carbon being C*n*1 and the para carbon being C*n*4.

it is possible that the chloride originated from CH_2Cl_2, which was used in the preparation of the $IrH_3(CO)(dppe)$ starting material, or from a contaminant in the dimethylsilane. In any case, its existence appears clear with an observed Si–Cl distance of 2.111 (4) Å, which agrees well with other reported values for Si–Cl. If the chlorodimethylsilyl ligand arose from a redistribution reaction, there exist precedents for such reactions involving M–Cl and Si–R (R = H, Ph, $SiMe_3$).[13b,16,34]

There are two Ir–Si distances that differ slightly but significantly. The shorter distance is 2.397 (2) Å and belongs to Ir–

---

(34) Chang, L. S.; Johnson, M. P.; Fink, M. J. *Organometallics* **1989**, *8*, 1369–71.

Table VII. Refined Positional and Isotropic Thermal Parameters and Their Estimated Standard Deviations for $IrH(SiHMe_2)(SiClMe_2)(CO)(dppe)$ (**2j**)

atom	*x*	*y*	*z*	*B*(eq), Å^2
Ir	−0.06341 (3)	0.23549 (2)	0.21926 (4)	2.55 (2)
Cl	0.2352 (4)	0.1289 (3)	0.4894 (5)	10.987 (3)
P1	−0.1834 (2)	0.2905 (2)	−0.0247 (3)	2.8 (1)
P2	0.0902 (2)	0.2854 (2)	0.1666 (3)	2.9 (1)
Si1	−0.2468 (2)	0.2299 (2)	0.2695 (3)	3.5 (1)
Si2	0.0598 (3)	0.1964 (2)	0.4771 (3)	4.1 (2)
O	−0.0375 (7)	0.0430 (6)	0.151 (1)	5.6 (5)
C1	−0.0790 (8)	0.3087 (6)	−0.118 (1)	3.4 (5)
C2	0.0153 (9)	0.3547 (6)	−0.002 (1)	3.6 (5)
C3	−0.0457 (8)	0.1185 (8)	0.173 (1)	3.4 (5)
C4	−0.284 (1)	0.1203 (8)	0.269 (1)	6.1 (7)
C5	−0.269 (1)	0.2867 (8)	0.443 (1)	5.3 (6)
C6	0.095 (1)	0.2866 (8)	0.615 (1)	5.2 (6)
C7	0.023 (2)	0.115 (1)	0.573 (2)	9 (1)
C11	−0.2833 (8)	0.3970 (6)	−0.052 (1)	3.2 (5)
C12	−0.286 (1)	0.4505 (7)	0.070 (1)	4.2 (6)
C13	−0.355 (1)	0.5343 (7)	0.046 (1)	5.2 (7)
C14	−0.420 (1)	0.5646 (7)	−0.100 (2)	5.3 (7)
C15	−0.416 (1)	0.5123 (9)	−0.220 (1)	5.1 (7)
C16	−0.347 (1)	0.4305 (7)	−0.197 (1)	4.1 (6)
C21	−0.2747 (9)	0.2211 (6)	−0.153 (1)	3.2 (5)
C22	−0.398 (1)	0.2356 (7)	−0.191 (1)	4.2 (6)
C23	−0.464 (1)	0.178 (1)	−0.285 (1)	5.9 (7)
C24	−0.406 (2)	0.108 (1)	−0.341 (1)	7 (1)
C25	−0.280 (2)	0.0921 (8)	−0.298 (1)	6.6 (8)
C26	−0.215 (1)	0.1477 (7)	−0.208 (1)	4.2 (6)
C31	0.175 (1)	0.3571 (7)	0.307 (1)	3.8 (6)
C32	0.293 (1)	0.3286 (6)	0.396 (1)	3.6 (5)
C33	0.349 (1)	0.3829 (8)	0.507 (1)	4.9 (6)
C34	0.288 (1)	0.4619 (9)	0.531 (1)	5.5 (7)
C35	0.170 (1)	0.4886 (7)	0.447 (1)	5.7 (7)
C36	0.111 (1)	0.4357 (7)	0.335 (1)	4.3 (6)
C41	0.2065 (8)	0.2127 (7)	0.108 (1)	3.0 (5)
C42	0.210 (1)	0.1260 (7)	0.093 (1)	4.7 (6)
C43	0.291 (1)	0.0727 (8)	0.032 (2)	6.6 (8)
C44	0.369 (1)	0.107 (1)	−0.010 (2)	6.5 (8)
C45	0.370 (1)	0.194 (1)	0.008 (1)	5.7 (7)
C46	0.288 (1)	0.2459 (7)	0.065 (1)	4.7 (6)
H0	−0.091 (5)	0.329 (3)	0.260 (5)	−1 (1)

Table VIII. Selected Intramolecular Distances (Å) for $IrH(SiHMe_2)(SiClMe_2)(CO)(dppe)$ (**2j**)[a]

Ir–C3	1.86 (1)	P2–C41	1.82 (1)
Ir–P1	2.343 (3)	P2–C2	1.83 (1)
Ir–P2	2.355 (3)	P2–C31	1.85 (1)
Ir–Si2	2.394 (3)	Si1–C5	1.87 (1)
Ir–Si1	2.418 (3)	Si1–C4	1.88 (1)
Ir–H0	1.49 (5)	Si2–C7	1.81 (2)
Cl–Si2	2.111 (6)	Si2–C6	1.88 (1)
P1–C11	1.82 (1)	O–C3	1.19 (1)
P1–C21	1.82 (1)	C1–C2	1.55 (1)
P1–C1	1.83 (1)		

[a] Estimated standard deviations in the least significant figure are given in parentheses.

Table IX. Selected Bond Angles (deg) for $IrH(SiHMe_2)(SiClMe_2)(CO)(dppe)$ (**2j**)[a]

C3–Ir–P1	97.8 (3)	C1–P1–Ir	106.6 (3)
C3–Ir–P2	106.9 (3)	C2–P2–C41	100.0 (4)
C3–Ir–Si2	88.9 (3)	C2–P2–C31	102.8 (4)
C3–Ir–Si1	89.4 (3)	C2–P2–Ir	106.6 (3)
P1–Ir–P2	83.8 (1)	C41–P2–C31	104.3 (5)
P1–Ir–Si2	173.3 (1)	C41–P2–Ir	122.1 (3)
P1–Ir–Si1	89.0 (1)	C31–P2–Ir	117.9 (3)
P2–Ir–Si2	93.6 (1)	C5–Si1–C4	106.8 (5)
P2–Ir–Si1	162.9 (1)	C5–Si1–Ir	117.3 (4)
Si2–Ir–Si1	91.8 (1)	C4–Si1–Ir	117.1 (4)
H0–Ir–C3	174 (2)	C7–Si2–C6	107.5 (7)
H0–Ir–P1	82 (2)	C7–Si2–Cl	97.2 (6)
H0–Ir–P2	79 (2)	C7–Si2–Ir	118.7 (5)
H0–Ir–Si2	92 (2)	C6–Si2–Cl	101.9 (4)
H0–Ir–Si1	84 (2)	C6–Si2–Ir	117.6 (4)
C21–P1–C11	104.5 (5)	Cl–Si2–Ir	110.7 (2)
C21–P1–C1	104.7 (4)	C2–C1–P1	107.1 (6)
C21–P1–Ir	117.4 (3)	C1–C2–P2	107.8 (7)
C11–P1–C1	99.8 (4)	O–C3–Ir	175.5 (8)
C11–P1–Ir	121.2 (3)		

[a] Estimated standard deviations in the least significant figure are given in parentheses.

$SiMe_2Cl$, while the longer value is 2.418 (1) Å for $Ir–SiHMe_2$. This difference is in accord with the effect of chloride as a substituent relative to hydride as discussed above. Other reported Ir–Si distances are for complexes that are sufficiently different as to preclude valid detailed comparison. For example, the $Ir–SiEt_3$ distance of 2.390 (1) Å is found in the Ir(V) complex $(C_5Me_5)IrH_2(SiEt_3)_2$,[35] while the average Ir–Si distance of 2.41 Å is observed for the strained chelating disiloxane in $IrH(Me_2SiOSiMe_2)(CO)(PPh_3)_2$.[36] While the hydride ligand was located in the structure determination, its distance from iridium appears shorter than expected (1.50 (5) Å). Because of large estimated standard deviations in the coordinates of the hydride ligand, we attach little significance to this Ir–H value or to the bond angles involving the hydride. The rest of the coordination sphere, however, clearly reflects its presence.

Reaction of $IrH(SiH_2Et)_2(CO)(dppe)$ with $BF_3{\cdot}Et_2O$. Stimulated by current interest in silicon–silicon bond formation as it relates to polysilane synthesis,[14,37] we briefly examined the reactivity of the bis(silyl)iridium complexes. There is no evidence for reductive elimination of a disilane product from these complexes. This reductive elimination process should be relatively high in energy, since the chelating dppe ligand spans the coordination sites trans to the silyl groups, thereby constraining the complex from forming the square-planar intermediate A upon cis reductive elimination. A Lewis acid was used in an attempt to prepare an iridium disilene complex from a bis(silyl) complex. The iridium disilene species would then have the potential to react further with additional silane. Transition-metal disilene complexes have recently been reported and have been found to be reactive toward small molecules.[38]

Reaction of $IrH(SiEtH_2)_2(CO)(dppe)$ (**2i**) with $BF_3{\cdot}Et_2O$ occurs in C_6H_6 at room temperature when the mixture is stirred for 24 h. The ^1H NMR spectrum of the colorless product is devoid of Si–*H* resonances but reveals the presence of a metal hydride, two ethyl groups apparently bonded to silicon, and a dppe ligand. The IR spectrum indicates a metal carbonyl trans to the hydride ligand. An X-ray structure determination of the product revealed the identity of the complex to be $IrH(SiEtF_2)_2(CO)(dppe)$ (**3**) with fluorides replacing hydrides as the substituents bonded to the silicon atoms.

Structure of $IrH(SiEtF_2)_2(CO)(dppe)$ (3). Figure 3 shows a perspective drawing of complex **3**, which has an octahedral coordination geometry with two $SiEtF_2$ ligands located trans to the dppe P donors. Table X contains the refined positional and isotropic thermal parameters for the structure, while Tables XI and XII contain selected bond distances and angles. The coordination geometry of **3** is essentially identical with that of **2d** and **2j**. In accord with the above discussion of Ir–Si distances, the Ir–Si distances in **3** are significantly shorter than those in **2d** and **2j** with an average value of 2.360 (10) Å. It is evident that the fluoride substituents increase the stability of the Ir–Si bond. While

---

(35) Ricci, J. S.; Koetzle, T. F.; Fernandez, M.-J.; Maitlis, P. M.; Green, J. C. *J. Organomet. Chem.* **1986**, *299*, 383.

(36) Curtis, M. D.; Green, J.; Butler, Wm. *J. Organomet. Chem.* **1979**, *164*, 371.

(37) (a) Aitken, C. T.; Harrod, J. F.; Samuel, E. *J. Organomet. Chem.* **1985**, *279*, C11. (b) Harrod, J. P.; Aitken, C. T. Presented at the International Chemical Congress of the Pacific Basin Societies, Honolulu, HI, 1984; Paper 7K12. (c) West, R. J. *J. Organomet. Chem.* **1986**, *300*, 327. (d) Aitken, C. T.; Harrod, J. F.; Samuel, E. *J. Am. Chem. Soc.* **1986**, *108*, 4059. (e) Zarate, E. A.; Tessier-Youngs, C. A.; Youngs, W. J. *J. Am. Chem. Soc.* **1988**, *110*, 4068.

(38) (a) Pham, E. K.; West, R. *J. Am. Chem. Soc.* **1989**, *111*, 7667–8. (b) Berry, D. H.; Chey, J. H.; Zipin, H. S.; Carroll, P. J. *J. Am. Chem. Soc.* **1990**, *112*, 452–3.

Table X. Refined Positional and Isotropic Thermal Parameters and Their Estimated Standard Deviations for IrH(SiEtF$_2$)$_2$(CO)(dppe) (3)

atom	x	y	z	B(eq), Å^2
Ir	0.25213 (5)	0.21041 (9)	0.10878 (3)	2.03 (5)
P1	0.1879 (4)	0.3893 (6)	0.1610 (2)	2.4 (2)
P2	0.1913 (4)	0.3526 (6)	0.0244 (2)	2.4 (2)
Si1	0.2766 (4)	0.0519 (8)	0.1905 (3)	3.4 (3)
Si2	0.2922 (5)	0.0172 (8)	0.0518 (4)	4.4 (3)
F1	0.210 (1)	0.082 (2)	0.2349 (7)	5.6 (8)
F2	0.289 (1)	0.063 (2)	−0.0167 (6)	8 (1)
F3	0.223 (1)	−0.112 (2)	0.040 (1)	12 (1)
F4	0.251 (1)	−0.114 (2)	0.1710 (8)	8 (1)
O	0.434 (1)	0.326 (2)	0.136 (1)	6 (1)
C1	0.368 (2)	0.279 (3)	0.127 (1)	4 (1)
C2	0.170 (1)	0.546 (2)	0.112 (1)	3 (1)
C3	0.125 (1)	0.492 (2)	0.0501 (9)	3 (1)
C4	0.384 (2)	0.027 (4)	0.243 (1)	7 (2)
C5	0.420 (3)	0.145 (5)	0.280 (2)	12 (3)
C6	0.411 (3)	−0.052 (5)	0.080 (1)	13 (3)
C7	0.425 (5)	−0.172 (8)	0.056 (3)	16 (2)
C11	0.078 (1)	0.361 (2)	0.173 (1)	3 (1)
C12	0.040 (2)	0.464 (2)	0.205 (1)	5 (1)
C13	−0.044 (2)	0.448 (3)	0.214 (1)	5 (1)
C14	−0.088 (2)	0.328 (3)	0.195 (1)	5 (1)
C15	−0.052 (2)	0.224 (3)	0.165 (1)	4 (1)
C16	0.030 (2)	0.240 (3)	0.154 (1)	4 (1)
C21	0.110 (1)	0.267 (2)	−0.036 (1)	3 (1)
C22	0.117 (2)	0.276 (3)	−0.097 (1)	3 (1)
C23	0.057 (2)	0.216 (3)	−0.137 (1)	4 (1)
C24	−0.017 (2)	0.147 (3)	−0.126 (1)	4 (1)
C25	−0.025 (2)	0.140 (3)	−0.063 (1)	5 (1)
C26	0.037 (2)	0.197 (3)	−0.023 (1)	4 (1)
C31	0.262 (1)	0.450 (2)	−0.0151 (9)	3 (1)
C32	0.238 (2)	0.577 (3)	−0.044 (1)	6 (1)
C33	0.287 (2)	0.649 (4)	−0.081 (1)	7 (2)
C34	0.370 (2)	0.588 (4)	−0.080 (1)	6 (2)
C35	0.397 (2)	0.468 (4)	−0.049 (2)	7 (2)
C36	0.346 (2)	0.399 (3)	−0.015 (1)	6 (2)
C41	0.251 (1)	0.453 (2)	0.232 (1)	3 (1)
C42	0.319 (2)	0.556 (3)	0.234 (1)	5 (1)
C43	0.370 (2)	0.603 (3)	0.288 (2)	6 (2)
C44	0.354 (2)	0.552 (4)	0.341 (2)	7 (2)
C45	0.292 (2)	0.455 (4)	0.341 (1)	7 (2)
C46	0.237 (2)	0.403 (3)	0.286 (1)	5 (1)

Table XI. Selected Intramolecular Distances (Å) for IrH(SiEtF$_2$)$_2$(CO)(dppe) (3)[a]

Ir–P1	2.380 (5)	Si1–F1	1.62 (1)
Ir–P2	2.368 (6)	Si1–F4	1.62 (2)
Ir–Si1	2.349 (7)	Si1–C4	1.86 (3)
Ir–Si2	2.372 (7)	Si2–F2	1.62 (2)
Ir–C1	1.87 (2)	Si2–F3	1.59 (2)
P2–C2	1.82 (2)	Si2–C6	1.93 (4)
P1–C11	1.81 (2)	O–C1	1.10 (2)
P1–C41	1.81 (2)	C2–C3	1.53 (3)
P2–C3	1.82 (2)	C4–C5	1.43 (5)
P2–C21	1.85 (2)	C6–C7	1.29 (8)
P2–C31	1.81 (2)		

[a] Estimated standard deviations in the least significant figure are given in parentheses.

the mechanism of silyl redistribution is unclear at this time, it is certain no movement toward Si–Si coupling was achieved in the reaction of IrH(SiEtH$_2$)$_2$(CO)(dppe) with BF$_3$·Et$_2$O.

Experimental Section

All procedures were performed in a nitrogen-filled glovebox, under nitrogen or another appropriate gas by using a Schlenk-type vacuum line, or on a high-vacuum line. Solutions for NMR samples were usually prepared in a glovebox and placed in resealable NMR tubes fitted with J. Young valves (Wilmad Glass Co.) or placed in NMR tubes attached to ground-glass joints and fitted with needle-valve adaptors for connection to a high-vacuum line. These NMR samples were connected to a high-vacuum line for freeze/pump/thaw cycles at −78 °C and/or exposure to gases, followed by sealing (or flame sealing). All solvents were reagent grade or better and were dried and degassed before use by accepted techniques.[39] The liquid-silane reagents (triethylsilane, dimethylchlorosilane, dichloromethylsilane, diphenylsilane, and phenylsilane (Petrarch Systems)) were degassed by freeze/pump/thaw cycles prior to their use. Most gases were used as received, including hydrogen (Air Products, 99.9%), deuterium (Air Products, 99.99%), carbon monoxide (Air Products, CP 99.3%), carbon-^{13}C monoxide (Monsanto Research Corporation, 99%), ethylene (Matheson, CP 99.5%), trimethylsilane, dimethylsilane, and ethylsilane.

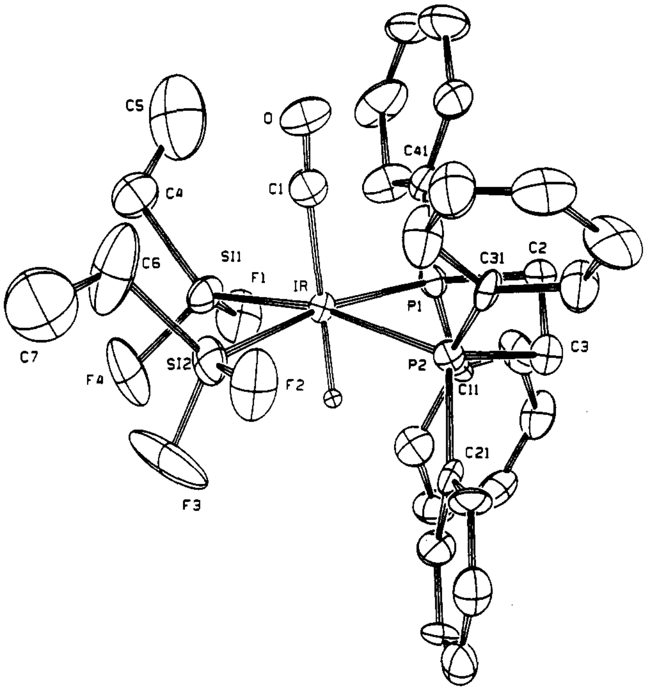

Figure 3. Perspective drawing of the coordination geometry of 3. The hydride ligand was not located in the actual structure determination. The phenyl carbon atoms are numbered sequentially with the ipso carbon being C*n*1 and the para carbon being C*n*4.

Table XII. Selected Bond Angles (deg) for IrH(SiEtF$_2$)$_2$(CO)(dppe) (3)[a]

P1–Ir–P2	83.5 (2)	C3–P2–C31	105 (1)
P1–Ir–Si1	92.7 (2)	C21–P2–C31	103 (1)
P1–Ir–Si2	170.5 (2)	Ir–Si1–F1	112.1 (6)
P1–Ir–C1	97.9 (8)	Ir–Si1–F4	112.2 (7)
P2–Ir–Si1	166.0 (2)	Ir–Si1–C4	125 (1)
P2–Ir–Si2	94.2 (2)	F1–Si1–F4	100.3 (9)
P2–Ir–C1	101.3 (7)	F1–Si1–C4	103 (1)
Si1–Ir–Si2	87.3 (3)	F4–Si1–C4	101 (1)
Si1–Ir–C1	92.6 (7)	Ir–Si2–F2	112.2 (6)
Si2–Ir–C1	91.6 (8)	Ir–Si2–F3	114.5 (7)
Ir–P1–C2	105.7 (7)	Ir–Si2–C6	114 (1)
Ir–P1–C11	119.2 (8)	F2–Si2–F3	99 (1)
Ir–P1–C41	118.2 (7)	F2–Si2–C6	104 (1)
C2–P1–C11	100 (1)	F3–Si2–C6	112 (2)
C2–P1–C41	106 (1)	Ir–C1–O	176 (2)
C11–P1–C41	105 (1)	P1–C2–C3	107 (1)
Ir–P2–C3	106.6 (7)	P2–C3–C2	111 (2)
Ir–P2–C21	118.0 (7)	Si1–C4–C5	119 (3)
Ir–P2–C31	120.4 (7)	Si2–C6–C7	112 (5)
C3–P2–C21	102 (1)		

[a] Estimated standard deviations in the least significant figure are given in parentheses.

^{1}H and ^{31}P NMR spectra were recorded at 400.13 and 161.98 MHz, respectively, on a Bruker WH-400 spectrometer. A Bruker BVT-1000 temperature control unit was used in the regulation of temperature when needed and was calibrated against standard methanol (low temperature) or ethylene glycol (high temperature) samples. ^{1}H chemical shifts are reported in ppm downfield from tetramethylsilane but were measured relative to residual ^{1}H resonances in the deuterated solvents, C$_6$D$_5$H (δ 7.150 ppm) and C$_6$D$_5$CD$_2$H (δ 2.100 ppm). ^{31}P chemical shifts are reported in ppm downfield from phosphoric acid and were referenced to

---

(39) Perrin, D. D.; Armarego, W. L. F.; Perrin, D. R. *Purification of Laboratory Chemicals*, 2nd ed.; Pergamon: New York, 1980.

external 85% H_3PO_4. Benzene-d_6 (MSD, 99.6% D) and toluene-d_8 (Aldrich, 99+% D) were vacuum distilled from sodium benzophenone ketyl solutions. Infrared spectra were recorded on a Mattson Sirius 100 FT-IR instrument. Elemental analyses were performed by Galbraith Laboratories, Inc., Knoxville, TN.

The complex $IrH_3(CO)(dppe)$ was prepared according to the literature procedure.[19]

Synthesis of 1a–i and 2c,e–j: Sealed NMR Tube Reactions. The complex $IrH_3(CO)(dppe)$ (0.002 g, 3.22×10^{-6} mol) was placed in an NMR tube, which was attached to a ground-glass joint. This tube was evacuated on the high-vacuum line, and C_6D_6 or toluene-d_8 was then condensed into the tube. For gaseous silanes, 400 Torr (10 cm^3) of the gas was then condensed onto the frozen solvent. For liquid silanes, the deuterated solvent was first condensed into the vessel containing the silane (7 μL), followed by vacuum transfer into the tube containing $IrH_3(CO)(dppe)$. The tube was then flame sealed. Heating the sealed tube in an oil bath at 60 °C for the appropriate length of time then produced the desired mono- or bis(silyl)iridium complex. All of the mono(silyl)iridium complexes were produced in 1.5 h or less (depending upon the electronegativity of the substituents on the silane). The bis(silyl)iridium complexes formed in times that ranged from 12 h for primary silanes to 2 weeks for Me_3SiH.

Synthesis of $IrH(Me_2SiCl)_2(CO)(dppe)$ (2d). $IrH_3(CO)(dppe)$ (0.030 g, 4.8×10^{-5} mol) was placed in a 10-mL vessel affixed with a high-vacuum stopcock and dissolved in 5 mL of benzene. Me_2ClSiH (0.5 mL) was placed in a 10-mL pear-shaped flask and was degassed by three freeze–pump–thaw cycles. Upon thawing, the silane was vacuum transferred onto the evacuated, frozen benzene solution. This mixture was then placed in an oil bath at 60 °C and stirred for 48 h. The colorless solution was then filtered through a fine glass frit and evaporated to dryness, leaving a pale tan powder. Yield of crude product: 0.038 g (97%). The product may be recrystallized from toluene/benzene by slow evaporation of solvent and formed as colorless blocks. Yield of recrystallized product: 0.035 g (90%). Anal. Calcd for $C_{31}H_{37}ClIrOP_2Si_2$: C, 46.26; H, 4.64. Found: C, 46.66; H, 4.54.

Synthesis of $IrH(EtSiF_2)_2(CO)(dppe)$ (3). The complex $IrH(EtSiH_2)_2(CO)(dppe)$ (0.030 g, 4.3×10^{-5} mol) was placed in a 25-mL flask equipped with an argon inlet and dissolved in 4 mL of benzene. To this stirred solution was injected $BF_3 \cdot Et_2O$ (20 μL, 0.163 mol). Evolution of gas was observed immediately and was greatest during the first 10 min of stirring. The pale tan solution was stirred for 5 h, filtered through a fine glass frit, and evaporated to dryness. The product was recrystallized from toluene/benzene by slow evaporation of solvent to yield colorless plates. Yield of recrystallized product: 0.020 g (65%).

Crystal Structure Determinations. The same general procedures were used for all of the structure determinations. A colorless crystal, attached to the end of a glass fiber, was mounted on a CAD4 κ-axis diffractometer. The peak search and centering routine was used to locate 25 reflections in different parts of reciprocal space. The CAD4 indexing program generated a unit cell, which was verified through the cell reduction program TRACER. Space group assignment was carried out by analyzing the intensity data for symmetry and systematic absences. Crystallographic data, experimental details, and refinement parameters for the crystal structure determinations are presented in Table I and in Table SI of the supplementary material. None of the intensity data sets showed evidence of decay during data collection.

All structures were solved by standard heavy-atom methods using a Patterson map, least-squares refinements, and a succession of difference Fourier maps to locate the non-hydrogen atoms. An empirical absorption correction was performed for each data set. Except as noted below, all non-hydrogen atoms were refined anisotropically in the final refinement model with hydrogen atoms placed at calculated positions. Attempts to locate the hydride ligand were only successful in the structure determination of **2j**. Tables of final refined positional and isotropic thermal parameters are given for each structure along with tables of selected bond distances and angles. Supplementary material contains the final anisotropic thermal parameters, calculated hydrogen positional parameters, complete tabulations of bond distances and angles, and a listing of observed and calculated structure factor amplitudes for each structure. See paragraph regarding supplementary material at the end of the paper.

Structure Determination of 2d. The structure of **2d** exhibited a rotational disorder of the Cl and methyl positions of the silyl group denoted by Si2. A satisfactory model was formulated and refined in which the Cl substituent occupied two positions to differing extents. The atom Cl2 was assigned a multiplicity of 0.8, while a second Cl atom, Cl3, was located near atom C6 and given a multiplicity of 0.2. The carbon atom C6 was assigned a multiplicity of 0.8, and both C6 and Cl3 were refined by using an isotropic thermal model. Not surprisingly, we were unable to see evidence of a carbon atom near Cl2, which, according to the model, would have a multiplicity of 0.2. Attempts to locate the hydride ligand were unsuccessful. The largest residual electron density on the final difference Fourier map was located near the Ir atom and corresponded to ca. 15% of the height of a carbon atom.

Structure Determination of 2j. Evidence for a Cl substituent on the silyl ligand denoted by Si1 was compelling even though the synthesis was performed in the apparent absence of Cl-containing materials. The relatively large isotropic thermal parameter for Cl is consistent with a less-than-full site occupancy, but no attempt was made to reduce the Cl multiplicity in order to get its thermal parameter in closer agreement with others in the structure. The hydride ligand was located and refined satisfactorily. However, as in any structure of a third transition series metal, parameters associated with an attached hydride should be viewed with caution.

Structure Determination of 3. The quality of the intensity data set was significantly poorer than those used for **2d** and **2j**, resulting in substantially higher final agreement factors (see Table III). One of the ethyl groups showed a disorder of the methyl carbon C7. An attempt to model the disorder proved inconclusive, and in the final refinement a single carbon atom was used with a multiplicity factor of 0.8. The final difference Fourier map showed its highest peaks corresponding to 15% of the height of a carbon atom within 1.4 Å of the iridium atom. Consequently, no attempt was made to locate the hydride ligand.

Acknowledgment. We wish to thank the National Science Foundation (Grants CHE 86-03055 and 89-09060) for support of this work and Johnson Matthey Co., Inc., for a generous loan of iridium trichloride. We also thank Prof. Don Berry for helpful comments and Brian Cleary for synthetic help.

Supplementary Material Available: For **2d**, **2j**, and **3**, Table SI, listing complete crystal data and intensity collection parameters for the structure determinations, and Tables SII–XIII, listing refined thermal parameters, calculated hydrogen positional parameters, and complete bond distances and angles (23 pages); tables of observed and calculated structure factor amplitudes (×10) (55 pages). Ordering information is given on any current masthead page.